

1 **Quantifying primary and secondary humic-like substances in**
2 **urban aerosol based on emission source characterization and a**
3 **source-oriented air quality model**

4 Xinghua Li¹, Junzan Han¹, Philip K. Hopke², Jingnan Hu³, Qi Shu¹, Qing Chang¹, Qi Ying⁴

5 ¹School of Space and Environment, Beihang University, Beijing, 100191, China

6 ²Center for Air Resources Engineering and Science, Clarkson University, Potsdam, NY USA.

7 ³State Environmental Protection Key Laboratory of Vehicle Emission Control and Simulation, Chinese Research
8 Academy of Environmental Sciences, Beijing 100012, China

9 ⁴Zachry Department of Civil Engineering, Texas A&M University, College Station, TX 77843, USA

10 *Correspondence to:* Xinghua Li (lixinghua@buaa.edu.cn); Qi Ying (qying@civil.tamu.edu)

11 **Abstract:** Humic-like substances (HULIS) are a mixture of high molecular weight, water-soluble organic compounds
12 that are widely distributed in atmospheric aerosol. Their sources are rarely studied quantitatively. Biomass burning is
13 generally accepted as a major primary source of ambient humic-like substances (HULIS) with additional secondary
14 material formed in the atmosphere. However, the present study provides direct evidence that residential coal burning is
15 also a significant source of ambient HULIS, especially in the heating season in northern China based on source
16 measurements, ambient sampling and analysis, and apportionment with source-oriented CMAQ modeling. Emissions
17 tests show that residential coal combustion produces 5 to 24% of the emitted organic carbon (OC) as HULIS carbon
18 (HULIS_c). Estimation of primary emissions of HULIS in Beijing indicated that residential biofuel and coal burning
19 contribute about 70% and 25% of annual primary HULIS, respectively. Vehicle exhaust, industry, and power plants
20 contributions are negligible. Average concentration of ambient HULIS in PM_{2.5} was 7.5 µg/m³ in urban Beijing and
21 HULIS exhibited obvious seasonal variations with the highest concentrations in winter. HULIS_c account for 7.2% of
22 PM_{2.5} mass, 24.5% of OC, and 59.5% of WSOC, respectively. HULIS are found to correlate well with K⁺, Cl⁻, sulfate,
23 and secondary organic aerosol suggesting its sources include biomass burning, coal combustion and secondary aerosol
24 formation. Source apportionment based on CMAQ modeling shows residential biofuel and coal burning, secondary
25 formation are important sources of ambient HULIS, contributing 47.1%, 15.1%, and 38.9%, respectively.

26

27 **1 Introduction**

28 Humic-like substances (HULIS) are a mixture of higher molecular weight organic compounds that resemble terrestrial
29 and aquatic humic and fulvic acids with similar structures and properties (Graber and Rudich, 2006). HULIS are widely
30 distributed in the atmospheric aerosol, rain, and cloud and fog droplets and account for a significant proportion of the
31 organic carbon and water-soluble organic carbon (WSOC). For example, Zheng et al. (2013) reported that 9% to 72% of
32 WSOC is HULIS. Because of their water-soluble and strong surface-active properties, HULIS may play an important
33 role in the formation of clouds as condensation nuclei, ice nuclei and through aerosol hygroscopic growth (Dinar et al.,
34 2006; Wang and Knopf, 2011; Gysel et al., 2004). Due to their strong light absorption in the UV range, HULIS can play
35 an active role as brown carbon in the radiative transfer and photochemical processes (Hoffer et al., 2006). HULIS
36 deposition can also lead to a decrease in the albedo of ice and snow surfaces (Beine et al., 2011; France et al., 2011;
37 France et al., 2012). Owing to their redox-active characteristics, HULIS was also suggested to induce adverse health
38 effect (Lin and Yu, 2011; Ghio et al., 1996; Verma et al., 2012).

39 In recent years, studies focusing on the spatial and temporal variations, sources, and formation of HULIS have been
40 reported. A summary of these studies is provided in Table S1. Previous studies have identified primary emission and
41 atmospheric secondary formation as the important sources of HULIS. Among the primary emission sources, biomass
42 burning is generally accepted as a major source of HULIS, with the evidence from ambient and source sampling as well
43 as source apportionment studies (Lin et al., 2010a, b; Kuang et al., 2015; Park and Yu, 2016; Schmidl et al., 2008a, b;
44 Goncalves et al., 2010). Recently, residential coal burning was suggested as an important primary HULIS source during
45 winter (Tan et al., 2016; Voliotis et al., 2017). However, direct evidence of HULIS emission from coal combustion is
46 limited. Only one study on HULIS emitted from residential coal combustion was reported and the results showed that
47 HULIS accounted for 5.3% of smoke PM_{2.5} (Fan et al., 2016). Unfortunately, only a light coal in the shape of
48 honeycomb briquette was tested that did not reflect the variety of coal types and forms actually being used for
49 residential heating and cooking in China. Another possible primary HULIS source is vehicle exhaust although there is
50 uncertainty in the importance of this source (El Haddad et al., 2009; Salma et al., 2007; Lin et al., 2010b; Kuang et al.,
51 2015). No direct evidence of primary HULIS in vehicle exhaust has been reported. Secondary processes, including
52 formation in the cloud droplets, heterogeneous or aerosol-phase reactions, can be important sources of HULIS (Lin et
53 al., 2010b; Zheng et al., 2013).

54 Previous studies of HULIS source identification were generally based on the relationship between HULIS and the
55 tracers for specific sources (such as K, levoglucosan, Cl⁻, etc.) (Voliotis et al., 2017; Tan et al., 2016; Lin et al., 2010;

56 Park and Son, 2016; Baduel et al., 2010). Those correlation analyses between HULIS and some species may provide
57 some information regarding possible source and formation of HULIS. However, they do not provide quantitative source
58 apportionments. To date, studies that quantitatively identify HULIS sources are limited (Kuang et al., 2015; Srivastava
59 et al., 2018). Kuang et al. (2015) applied positive matrix factorization (PMF) to apportion sources of ambient HULIS in
60 the Pearl River Delta (PRD) in Southern China. Their study showed that secondary formation was the most important
61 source of HULIS throughout the year with an annual average contribution of 69% at an urban site. Biomass burning
62 also contributed significantly to ambient HULIS.

63 Thus, information is scarce on the quantitative apportionment of HULIS sources in the more polluted regions in
64 Northern China, especially in the winter when large quantities of coal are consumed for indoor heating. Moreover, a
65 considerable proportion of coal is burned in residential household stoves in rural, suburban and even some urban areas
66 under poor combustion conditions and without any emission controls. This coal combustion results in high air pollutant
67 emissions and high ambient concentrations. Wang et al. (2016) estimated that more than 30 million tons of coal are
68 burned per year in households in just the Beijing, Tianjin, and Hebei (BTH) region in Northern China. Residential
69 sources in the BTH region contributed to 32% and 50% of primary PM_{2.5} emissions over the whole year and in winter,
70 respectively (Liu et al., 2016).

71 The primary goals of this study are to determine whether residential coal combustion is a significant source of ambient
72 HULIS and quantify its contributions to HULIS in Beijing. Given the large vehicle population in Beijing (up to 5.2
73 million in 2012), this study also provides a chance to examine the vehicular emissions contribution to ambient HULIS.
74 Studies included: (1) Characterization of the HULIS emitted from residential coal stoves, vehicle exhaust, and
75 residential biofuel burning; (2) Estimation of anthropogenic primary emission of HULIS based on these source
76 measurements; (3) Measurement of HULIS concentrations and other major species in the ambient urban Beijing PM_{2.5}
77 from June 2012 to April 2013; and (4) Application of the source-oriented Community Multiscale Air Quality (CMAQ)
78 model to quantitatively determine the source contributions to HULIS. The information obtained in this study improves
79 our understanding of the characteristics and sources of primary HULIS and the impact of those sources on HULIS in
80 ambient PM_{2.5}.

81 **2 Materials and Methods**

82 **2.1 Ambient sampling**

83 Beijing is surrounded by mountains to the west, north, and northeast, and is adjacent to the northwest portion of the
84 North China Plain. It has a warm and semi-humid continental monsoon climate with four distinctive seasons,

85 characterized by strong windy and dusty weather in spring, high temperatures and humidity with extensive rain in
86 summer, cool and pleasant weather in autumn, and cold and dry weather in winter. The annual average wind speed is
87 2.5 m s^{-1} with mostly northerly or northwesterly winds in winter and southerly or southeasterly winds in summer.
88 Twenty-four-hour ambient $\text{PM}_{2.5}$ samples were collected non-continuously from 14 June 2012 to 2 April 2013 on the
89 campus of Beihang University (BHU, $39^{\circ}59'N$, $116^{\circ}21'E$) (Figure S1). The sampling period covered four seasons with
90 132 samples being collected for HULIS analysis. The site is surrounded by educational and residential districts without
91 major industrial sources. Major nearby roads are the North Fourth Ring Road about 900 m to the north, North Third
92 Ring Road about 1.2 km to the south, and Xueyuan Road about 350 m to the east. Ambient $\text{PM}_{2.5}$ sampling instruments
93 were installed on the roof of a building approximately 25 m above the ground level at Beihang University. A
94 high-volume aerosol sampler (RFPS-1287-063, Thermo, USA) was operated at a flow rate of $1.13 \text{ m}^3 \text{ min}^{-1}$ to collect
95 $\text{PM}_{2.5}$ samples on prebaked quartz filters (with area 417.6 cm^2) for the determination of water-soluble organic carbon
96 (WSOC) and humic-like substances (HULIS). $\text{PM}_{2.5}$ samples were also collected using a 5-channel Spiral Ambient
97 Speciation Sampler (SASS, Met One Inc., USA) with a flow rate of 6.7 L min^{-1} . Wang et al. (2015) provided the details
98 of the sample collection.
99 Meteorological data including wind speed (WS), temperature, relative humidity (RH) and precipitation were obtained
100 from China Meteorological Data Sharing Service System (<http://cdc.cma.gov.cn/home.do>).

101 **2.2 Source Sampling**

102 Residential biofuel and coal combustion emissions, and vehicle exhaust, which are representative of typical emission
103 sources around Beijing, were sampled in this study.

104 **2.2.1 Residential biofuel and coal combustion**

105 Three typical types of biofuel, i.e. wheat straw, corn stover, and wood, were burned in an improved stove, which has an
106 enclosed combustion chamber and a bottom grate and a chimney. The sampling procedures are described by Li et al.
107 (2007, 2009) and are briefly summarized here. The water boiling test was used to simulate a common cooking
108 procedure. The burning cycle included heating a specific amount of water from room temperature to its boiling point
109 and then letting it simmer for a few minutes. Both the high power and low power phases were included in the burn
110 cycle to simulate cooking practices of a typical household. The sampling period covered the entire cycle and lasted
111 20-30 minutes.

112 Five coal types were selected for source testing covering a wide range of maturity with volatile matter content varying
113 from 9.6% to 32.4%. Two coal stoves were tested, including a high efficiency, heating stove that employs under-fire

114 combustion technology and a traditional cooking and heating stove that employs over-fire combustion technology (Li et
115 al., 2016). Four chunk coals and one briquette coal were burned in the high efficiency stove and three chunk coals were
116 burned in the traditional stove. Coal/stove combinations are presented in Table 2. To reduce the interference from
117 igniting the fire, coal was ignited with a propane gas flame from a torch. Emission sampling covered from fire start to
118 fire extinction and lasted two to three hours.

119 Source testing of residential biofuel and coal combustion was performed at Beihang University. The test fuels were
120 air-dried, and the results of their proximate and ultimate analyses are listed in Table S2 in the Supplement. An outline of
121 the sampling system is shown in Fig. S2. The stove was placed into a chamber. Purified air was introduced into the
122 chamber with a fan to provide dilution air. Emissions were extracted from the chimney with an exhaust hood and were
123 diluted with purified air, cooled to no more than 5 degrees Celsius at ambient temperature, and then drawn through a
124 sampling duct and exhausted from the laboratory. Both air flows were adjusted using frequency modulators to change
125 fan speeds. The gas flow velocity in the sampling duct was measured by a pitot tube to be over 5 m/s. Flow was
126 isokinetically withdrawn from the sampling duct with a probe and directed into the residence chamber. PM_{2.5} samples
127 were collected from the end of the residence chamber onto prebaked quartz filters with a diameter of 47mm through
128 PM_{2.5} cyclones at a flow rate of 16.7 liters/min.

129 **2.2.2 Vehicle exhaust**

130 Four light-duty gasoline vehicles certified as meeting the China 4 emissions regulations were tested for their emissions
131 on a chassis dynamometer. The tests were conducted using the New European Driving Cycle (Marotta, et al., 2015) and
132 lasted 1180 s, including four repeated urban driving cycles and one extra-urban driving cycle. The emissions testing and
133 sampling system are described in detail by Li et al. (2016) and are briefly summarized here. The vehicle exhaust was
134 directed into a critical flow Venturi constant volume sampler in a full flow dilution tunnel. The PM_{2.5} samples were
135 collected on prebaked quartz filters with a diameter of 47mm through PM_{2.5} cyclones at a flow rate of 80 L/min.

136 Three heavy-duty diesel trucks were selected to perform on-road emission tests. The tests were conducted on both
137 highway and city roads. The emission testing and sampling system are described in detail elsewhere (He et al., 2015)
138 and are briefly summarized here. A Micro Proportional Sampling System (SEMTECH-MPS; Sensors Inc., MI, USA)
139 was used to draw a constant ratio of sample flow to exhaust flow and dilute the sample flow. PM_{2.5} samples were
140 collected onto prebaked quartz filters with a diameter of 47mm through PM_{2.5} cyclones at a flow rate of 10 liters/min.
141 Tunnel measurements were also conducted to collect vehicle exhaust at the Badaling Tunnel in Beijing. The length of
142 the tunnel is 1085 m. The ventilation in the tunnel was achieved by the flow of the traffic induced into the tunnel during
143 the sampling period. PM_{2.5} samplers with prebaked 47mm quartz filters were operated at a flow rate of 16.7 L/min at

144 the inlet and the outlet of the tunnel simultaneously. The sampling period was 2 hours and the samples represent the
145 mixed exhaust of gasoline-fueled vehicles and diesel-fueled vehicles.
146 All source samples collected on the quartz filters were analyzed for HULIS, WSOC and OC/EC according the methods
147 described in Section 2.3.

148 **2.3 Chemical Characterization**

149 HULIS isolation was based on the extraction method developed by Varga et al. (2001) and used in many other studies
150 (Nguyen et al., 2014; Lin et al., 2010b; Fan et al., 2012; Song et al., 2012; Lin et al., 2011; Salma et al., 2013; Feczko et
151 al., 2007; Krivácsy et al., 2008). The separation procedure is provided in Text S1 of the Supplement. WSOC and
152 HULIS_C were determined using a total organic carbon (TOC) analyzer (Shimadzu TOC-Vcph, Japan) based on a
153 combustion-oxidation, non-dispersive infrared absorption method. The TOC was determined by subtracting inorganic
154 carbonate (IC) from total carbon (TC): $TOC = TC - IC$. The reported data were the average results of three replicate
155 measurements. Mass concentrations of HULIS were obtained from HULIS_C by multiplying a scaling factor of 1.9 as
156 suggested by Lin et al. (2012a), Kiss et al. (2002), and Zheng et al. (2013).

157 A 0.5 cm² punch from each quartz filter was analyzed for OC and EC using a DRI Model 2001 Thermal/Optical Carbon
158 Analyzer (Atmoslytic Inc., Calabasas, USA) following the IMPROVE-A thermal optical reflectance (TOR) protocol
159 (Chow et al., 2007).

160 The PM_{2.5} samples from SASS were also analyzed for mass, water-soluble inorganic ions analysis as described by
161 Wang et al. (2015).

162 **2.4 CMAQ modelling of primary HULIS_C**

163 A source-oriented version of the Community Multiscale Air Quality (CMAQ) model (version 5.0.1) was used in this
164 study to track primary PM_{2.5} (PPM_{2.5}) from different emission sectors and determine the resulting concentrations of
165 primary HULIS. The model was used in a previous study to determine source contributions to PPM_{2.5} mass, EC and
166 primary OC (POC) in China. Details of the source apportionment technique can be found in Hu et al (2015). In
167 summary, source contributions to PPM_{2.5} mass were directly determined using non-reactive source-specific tracers to
168 track the emissions of PPM_{2.5} from different sources. These non-reactive tracers were treated identically to the other
169 PPM components when simulating their emission, transport, and removal. A constant scaling factor (typically 10⁻⁴ or
170 10⁻⁵) was used to scale the actual emission rate of these tracers to ensure that their concentrations are sufficiently low
171 that they do not alter the removal rates of other PM components. The concentrations and source contributions to EC and
172 POC were determined during post-processing by using source-specific emission factors as well as the model predicted

173 source contributions to $PPM_{2.5}$ mass concentrations. This technique can be used to determine source contributions to
174 primary HULIS. For example, contributions of the i^{th} emission source to primary HULIS concentration ($HULIS_{c,i}$) can
175 be calculated using equation (1):

$$176 \quad HULIS_{c,i} = PPM_{2.5,i} * f_{OC,i} * f_{HULIS,i} \quad (1)$$

177 where $f_{HULIS,i}$ is the mass fraction of HULIS per unit emission of POC from the i^{th} source (see Section 3.3 below for
178 estimation of HULIS primary emission) and $f_{OC,i}$ is the mass fraction of POC per unit emission of $PPM_{2.5,i}$ from the i^{th}
179 source, and $PPM_{2.5,i}$ is the calculated source contribution to $PPM_{2.5}$ from the i^{th} source based on the non-reactive tracer.
180 The total concentration of primary HULIS can be determined by adding the primary HULIS contributions from the
181 different sources.

182 In this study, the model uses a $36 \text{ km} \times 36 \text{ km}$ horizontal resolution to cover a rectangular domain that includes all of
183 China and neighboring countries. Source contributions to HULIS were calculated for the periods when observations of
184 HULIS are available. Emissions from anthropogenic source sectors (residential sources, power plants, industries, and
185 transportation) are based on Multi-resolution Emission Inventory of China (MEIC) 2012 (www.meicmodel.org). Open
186 biomass burning was estimated using the FINN dataset from the National Center for Atmospheric Research (NCAR)
187 (Wiedinmyer et al., 2011). Natural emissions from soil erosion and sea spray were modeled within the CMAQ model
188 (Appel et al., 2013; Kelly et al., 2010). Biogenic emissions were estimated using the Model for Emissions of Gases and
189 Aerosol from Nature (MEGAN) version 2.10. Meteorological fields were calculated using the Weather Research and
190 Forecasting (WRF) model. Details of the model setup, input data preparation, as well as model evaluation for $PPM_{2.5}$
191 mass are documented by Hu et al (2015). In this study, a comparison of predicted daily $PPM_{2.5}$ concentrations with
192 observations was performed and only those predictions with fractional errors (FE) less than 0.6 were included in the
193 calculation of primary HULIS. The values of f_{OC} for different source sectors used in the calculation are included in
194 Table S4 of the Supplement. These values were used in Ying et al. (2018), and the predicted daily-average POC and EC
195 concentrations generally agree with predictions for both daily and annual average concentrations.

196 **3 Results and discussion**

197 **3.1 General characteristics of ambient aerosol**

198 The concentrations of $PM_{2.5}$, carbonaceous species (OC, EC, WSOC and HULIS), and inorganic ions such as SO_4^{2-} ,
199 NO_3^- , NH_4^+ , and K^+ are summarized in Table 1. The 24-hour average $PM_{2.5}$ concentration for the sample set was $106 \pm$
200 $89 \mu\text{g}/\text{m}^3$, about three times the national annual air quality standard ($35 \mu\text{g}/\text{m}^3$). The highest concentration ($\sim 600 \mu\text{g}/\text{m}^3$)
201 appeared on 12-13 January 2013 as reported in other studies (Quan et al., 2014; Tian et al., 2014; Zheng et al., 2015).

202 The severe pollution events were always accompanied by high relative humidity and low wind speeds (Fig. 1). During
203 the entire sampling period, severely polluted days ($PM_{2.5}$ concentrations $\geq 150 \mu\text{g}/\text{m}^3$) constituted about 22%, while fair
204 days ($PM_{2.5}$ concentrations $\leq 75 \mu\text{g}/\text{m}^3$) approached 50%. The average $PM_{2.5}$ concentrations in summer, autumn, winter,
205 and spring were $98 \pm 60 \mu\text{g}/\text{m}^3$, $58 \pm 48 \mu\text{g}/\text{m}^3$, $150 \pm 121 \mu\text{g}/\text{m}^3$, and $120 \pm 76 \mu\text{g}/\text{m}^3$, respectively.

206 The average HULIS concentration for the study period was $7.5 \pm 7.8 \mu\text{g}/\text{m}^3$. This value is lower than the average
207 value of $11.8 \mu\text{g}/\text{m}^3$ measured at a rural site in the PRD region that was heavily influenced by biomass burning (Lin et
208 al., 2010b). However, it is higher than those measurements in the urban areas (about $5 \mu\text{g}/\text{m}^3$) in the PRD (Lin et al.,
209 2010a; Kuang et al., 2015), urban Shanghai (about $4 \mu\text{g}/\text{m}^3$) (Zhao et al., 2015), and urban Lanzhou (about $4.7 \mu\text{g}/\text{m}^3$)
210 (Tan et al., 2016). HULIS exhibited obvious seasonal variations as shown in Figure 1 and Table 1. The seasonal average
211 concentrations were $5.5 \pm 4.4 \mu\text{g}/\text{m}^3$, $5.6 \pm 4.7 \mu\text{g}/\text{m}^3$, $12.3 \pm 11.7 \mu\text{g}/\text{m}^3$, and $6.5 \pm 5.5 \mu\text{g}/\text{m}^3$ in summer, autumn,
212 winter, and spring, respectively. The winter mean was about twice the value in any other season, and the highest
213 concentration ($54.96 \mu\text{g}/\text{m}^3$) of HULIS was observed on the same day that the highest concentration of $PM_{2.5}$ was
214 observed. The mean HULIS concentrations were very similar between summer and autumn in contrast with $PM_{2.5}$ that
215 has much higher concentrations in the summer (Table 1). These seasonal variations were similar to those observed in
216 Aveiro and K-puszt (Fekko et al., 2007), but those annual average concentrations (about $2.4 \mu\text{g}/\text{m}^3$ and $3.2 \mu\text{g}/\text{m}^3$,
217 respectively) were much lower than in Beijing. The concentrations of HULIS in previously reported studies are
218 summarized in Table S1 of the Supplement.

219 HULIS and $PM_{2.5}$ had a significant correlation with the annual $r^2=0.90$ ($r^2 = 0.77, 0.96, 0.96$ and 0.94 in summer,
220 autumn, winter, and spring, respectively) (Figure S4a). The seasonal average of HULIS/ $PM_{2.5}$ was 5.9%, 9.4%, 7.9%,
221 and 4.8% in summer, autumn, winter, and spring, respectively. The annual average of HULIS/ $PM_{2.5}$ was $7.2\% \pm 3.3\%$,
222 and was approximately 10% lower than that in the PRD region (Lin et al., 2010a).

223 Strong correlations of HULIS_C with OC were observed, with the annual $r^2=0.87$ ($r^2 = 0.94, 0.82, 0.89$ and 0.84 in
224 summer, autumn, winter, and spring, respectively) (Fig S4c). The percentage of HULIS_C in OC for summer, autumn,
225 winter, and spring, respectively, were $29.2 \pm 6.2\%$, $26.2 \pm 9.6\%$, $21.0 \pm 7.1\%$, and $22.0 \pm 6.9\%$ with an annual average
226 of $24.5\% \pm 8.3\%$.

227 Strong correlations of HULIS_C with WSOC were also observed, with the annual $r^2=0.98$ ($r^2 = 0.99, 0.96, 0.99$ and 0.98
228 in summer, autumn, winter, and spring, respectively) (Figure S4b). The percentage of HULIS_C in WSOC for summer,
229 autumn, winter, and spring, respectively, were $66.7 \pm 5.4\%$, $54.1\% \pm 11.2\%$, $62.3\% \pm 5.7\%$ and $56.6\% \pm 6.3\%$, with an
230 annual average of $59.5\% \pm 9.2\%$, suggesting that HULIS_C was the major constituent of WSOC. This value is
231 comparable to the results (about 60%) at urban sites in the PRD region (Lin et al., 2010b; Fan et al., 2012), Shanghai

232 (Zhao et al., 2015), Korea (Park et al., 2012), Budapest (Salma et al., 2007; 2008; 2010), and high-alpine area of the
233 Jungfrauoch, Switzerland (Krivácsy et al., 2001). However, it is higher than the rural areas in K-puszta, Hungary
234 (Salma et al., 2010) and the northeastern US (Pavlovic and Hopke, 2012). The ratios of HULIS_C/WSOC reported by
235 previous studies are listed in Table S1 of the Supplement.

236 **3.2 HULIS emission characteristics from various sources**

237 The measured HULIS_C/OC (i.e. $f_{\text{HULIS},i}$), HULIS_C/WSOC from the source samples are presented in Table 2. Biomass
238 combustion produces a significant fraction of HULIS in OC (0.41-0.50) whether burning wood or crop straw. Those
239 values are high compared to previous studies (see Table S3 of the Supplement). The HULIS_C/OC values obtained by
240 Lin et al., (2010a, 2010b) were 0.14 to 0.34 from rice straw and sugarcane open burning in the PRD region in south
241 China. Park and Yu (2016) found the ratios from open burning rice straw, pine needles, and sesame stems in Korea were
242 in the range of 0.15 to 0.29. Schmidl et al. (2018a, 2018b) reported the ratios of 0.01-0.12 for wood burned in the stove
243 and 0.33-0.35 for leaves open burning in the mid-European Alpine region. Goncalves et al. (2010) obtained ratios of
244 0.04 to 0.11 from wood burned in the stove in Portugal. HULIS is an important component of water soluble organic
245 matter (WSOM). High HULIS_C/WSOC ratios (0.62 to 0.65) were observed for three types of biomass burning in this
246 study. These results are comparable with two previous studies. Fan et al. (2017) reported the ratios from open burning
247 rice straw, corn straw, and pine branch were in the range of 0.57 to 0.66. Park and Yu (2016) obtained ratios in the range
248 of 0.36 to 0.63 from open burning three types of biomass. However, Lin et al. (2010a) reported relatively low values
249 ranging from 0.30 to 0.33 from open burning rice straw and sugarcane. Possible influence factors to HULIS_C/OC ratios
250 were summarized in Table S3 of the Supplement. Combustion conditions have much influence on the HULIS-to-OC
251 ratios. For biomass open burning, HULIS-to-OC ratios varied less (from 0.14-0.35), while for biomass burned in the
252 stove, ratios varied a lot (from 0.01-0.50). For those advanced stoves used in European (with secondary air),
253 combustion is relatively complete, thus HULIS was generated less (0.01-0.12). While for the stoves used in Chinese
254 rural households, combustion is relatively inadequate, thus HULIS was generated more (0.41-0.50). Dilution ratio (DR)
255 and residence time (RT) could affect gas-particle partitioning, and thus have effect on the HULIS-to-OC ratios (Lipsky
256 et al., 2006; May et al., 2013). Moisture content of fuels was found to be not correlated with HULIS-to-OC ratios.
257 Residential coal combustion produces 5 to 24% of the OC as HULIS for all the coal/stove combinations in this study.
258 Only one prior study measured HULIS emitted from residential honeycomb coal briquette combustion (Fan et al., 2016).
259 However, the HULIS to OC ratio was not reported in that study. HULIS/WSOM ratio (0.46) in that study are
260 comparable with our HULIS_C/WSOC data (0.41-0.62).
261 Light-duty gasoline and heavy-duty diesel vehicles also produced primary HULIS on the order of 5 to 16% of the

262 emitted OC. The HULIS content detected in the vehicle exhaust samples was generally less than the detection limit for
263 these measurements. Thus, these reported ratios of HULIS_C to OC for vehicle emissions have high uncertainties. Ratios
264 of HULIS_C to OC for vehicle emissions obtained in this study are much higher than prior tunnel measurements (2-5%)
265 (El Haddad et al. 2009). However, they are comparable with those from residential coal combustion. Due to more
266 complete combustion or more advance emission controls in vehicles than residential solid fuel combustion, OC
267 emission factors for vehicles are normally around two orders of magnitude less than that for residential coal combustion
268 (MEP of China, 2014), so HULIS emission from vehicles can be neglected as described in Section 3.3.

269 **3.3 Estimation of HULIS primary emission**

270 The average values of $f_{\text{HULIS},i}$ for residential biofuel and coal combustion, and vehicle exhaust obtained from our
271 measurement were used for to assess the extent of primary emissions. Due to lack of the information of $f_{\text{HULIS},i}$ for the
272 other sectors, such as power plants and industries, considering combustion/production technology and emission control
273 technology, we assumed values for these two sectors as 0.01 and 0.05, respectively.

274 Based on OC emissions for different sources in the MEIC inventory and the $f_{\text{HULIS},i}$ for the various sources described
275 above, the annual anthropogenic primary emission of HULIS in Beijing is estimated to be approximately 6.3 Gg with
276 over 60 percent of this primary HULIS being emitted during the heating season. Residential biomass and coal burning
277 contribute about 70% and 25% of the annual primary HULIS emissions, respectively. Vehicle exhaust contributions to
278 annual primary HULIS emission are negligible (less than 2%). While industry sector and power plants contribute about
279 3% and close to zero of the annual primary HULIS emissions, respectively. In winter, residential biomass and coal
280 burning contribute close to 98 percent of primary HULIS (Table S5 of the Supplement).

281 Terrestrial and marine emissions were not included in these estimations of primary HULIS emissions since they were
282 considered to be negligible for inland cities, such as Beijing (Graber and Rudich, 2006; Zheng et al., 2013). Cooking
283 contributes about twenty percent of ambient fine organic aerosols in Beijing (Wang et al., 2009; Zhang et al., 2016; Sun
284 et al., 2016). Since cooking emissions was not included in MEIC, and no HULIS emission information about cooking is
285 available, thus cooking is not considered in the current model. It might make a contribution to ambient HULIS and need
286 to be explored in the future.

287 **3.4 Possible primary sources of HULIS**

288 Ambient HULIS sources include primary sources and atmospheric secondary processes that convert gaseous precursors
289 to HULIS. The correlation between HULIS and other measured constituents provide information regarding possible
290 sources and formation mechanisms of HULIS.

291 Correlations between HULIS and primary species in $PM_{2.5}$ are shown in Figure 2. POC and secondary organic carbon
292 (SOC) were estimated using the EC tracer method (Lim and Turpin, 2002; Turpin and Huntzicker, 1995). The details of
293 the method and evaluation are provided in Text S2. Figures 2a and 2b show that there are strong correlations between
294 HULIS and POC, and HULIS and EC throughout the year indicating that HULIS has sources and/or transport processes
295 similar to those of POC and EC. Both POC and EC are co-emitted by the incomplete combustion of carbon-containing
296 fuels. Thus, the correlation of HULIS with POC would be expected given its correlation with EC and the correlation
297 between EC and POC. According to the 2010 MEIC data for Beijing 2010, biomass and residential coal burning
298 contribute more than 80 percent of the POC emissions, the industrial sector contributes over 10 percent, and vehicular
299 exhaust contributions are negligible. For EC emission, residential coal burning contributes more than 50 percent,
300 biomass burning, industry, and vehicles contribute the rest.

301 K^+ generally originates from biomass burning with lesser contributions from coal burning and dust. However, biomass
302 burning is regarded as the most important source for K^+ and it is often used as an indicator of biomass burning (Kuang
303 et al., 2016; Zhang et al., 2013; Park et al., 2015; Pio et al., 2008; Wang et al., 2011; 2012; Cheng et al., 2013). In North
304 China, biomass burning occurred in all seasons including residential cooking, heating, and open biomass burning
305 (Cheng et al., 2013; Zheng et al., 2015). High K^+ concentrations in this study were observed with mean values of $2.2 \pm$
306 $2.9 \mu\text{g}/\text{m}^3$, $1.3 \pm 1.0 \mu\text{g}/\text{m}^3$, $3.2 \pm 3.6 \mu\text{g}/\text{m}^3$ and $2.2 \pm 1.3 \mu\text{g}/\text{m}^3$ in summer, autumn, winter, and spring, respectively,
307 and an annual average of $2.2 \pm 2.6 \mu\text{g}/\text{m}^3$. As shown in Figure 3c, HULIS and K^+ exhibited a strong correlation with
308 $r^2=0.76$, 0.73 , and 0.61 in summer, autumn, and spring, respectively, suggesting the contribution of biomass burning to
309 HULIS. During the winter sampling period, a low correlation was initially obtained ($r^2 = 0.21$). However, two extreme
310 values of K^+ were observed on New Year's Eve (February 9, 2013, $14.6 \mu\text{g}/\text{m}^3$) and Lantern Festival (February 24, 2013,
311 $17.6 \mu\text{g}/\text{m}^3$). Prior studies had suggested that fireworks during the Spring Festival and Lantern Festival produce very
312 high K^+ concentrations (Shen et al., 2009; Jing et al., 2014; Jiang et al., 2015). Excluding these two days (red points in
313 Figure 2c), the correlation between HULIS and K^+ increased to $r^2=0.73$, indicating the contribution of biomass burning
314 to HULIS in winter. The strong correlation coefficient between HULIS and K^+ across all the seasons also confirmed that
315 biomass burning was a significant primary HULIS emission source as presented in the Section 3.3.

316 Cl^- is usually believed to be associated with coal combustion and biomass burning (Yu et al., 2013; Gao et al., 2015;
317 Yao et al., 2002; Li et al., 2007; Li et al., 2009). A significant contribution from sea-salt particles for Cl^- in $PM_{2.5}$ can be
318 excluded since the average mole ratios of Cl^- to Na^+ across four seasons in this study is 5.0, much higher than the ratio
319 in seawater of 1.17. Moreover, the sampling site in Beijing is about 200 kilometres from the sea. The correlation of
320 HULIS and Cl^- is shown in Fig. 2d. In winter and spring, HULIS is moderately correlated with Cl^- with $r^2=0.56$ and

321 $r^2=0.64$, respectively. While weaker correlations between HULIS and Cl^- were observed in summer and autumn with
322 $r^2=0.40$ and $r^2=0.43$, respectively. This result reflects the different amounts of coal burned in specific seasons. In winter
323 and spring in northern China, coal combustion for heating was quite prevalent and more coal was burned compared to
324 the other two seasons, resulting in the substantial emissions of gaseous and particulate pollutants, including HULIS and
325 Cl^- . The correlation coefficient between HULIS and Cl^- in winter and spring provides additional support for coal
326 burning being an important primary HULIS emission source as discussed in Section 3.3. The strong correlation between
327 HULIS and Cl^- in winter ($r^2=0.89$) and weak correlation in summer ($r^2=0.17$) were also revealed in Lanzhou, another
328 city in northern China (Tan et al., 2016). Significant correlations between HULIS and Cl^- in wintertime urban aerosols
329 from central and southern Europe were also found (Voliotis et al., 2017). The authors suggest the high concentration of
330 HULIS during winter was probably related with residential coal burning (Tan et al., 2016; Voliotis et al., 2017).
331 Ca^{2+} would be more likely originated from the re-suspended road dust and long-range transported dust (Gao et al.,
332 2014). The poor correlation between HULIS and Ca^{2+} (as shown in Figure 2e) indicated dust was not likely to be an
333 important source of HULIS.

334 **3.5 HULIS source apportionment based on CMAQ modelling**

335 CMAQ predicted concentrations of $\text{PPM}_{2.5}$ from different sources were used to calculate HULISc from these sources
336 using equation (1). The total concentration of primary HULIS can be determined by adding up primary HULIS from
337 different sources. Figure 3 shows the predicted primary HULISc and observed HULISc concentrations with the
338 prediction uncertainty. Only days with acceptable $\text{PPM}_{2.5}$ performance were shown in the Figure 3. Primary HULISc in
339 January and March 2013 accounts for almost all observed HULISc in these two months. In summer and autumn 2012,
340 predicted primary HULISc concentrations are approximately $1\text{-}2 \mu\text{g m}^{-3}$. There were days when the observed HULISc
341 concentrations were much higher than the predicted primary HULISc concentrations indicating potential contributions
342 of secondary HULISc.

343 Table 3 shows the seasonal contributions for each source as well as average source contributions for the whole sampling
344 period to ambient HULIS in Beijing based on the observed total HULISc and CMAQ predicted primary HULISc on the
345 days with acceptable $\text{PPM}_{2.5}$ performance. Contributions of HULISc from secondary processes were determined by
346 subtracting predicted primary HULISc from observed HULISc. For those days when the predicted primary HULISc
347 concentrations are greater than the observed HULISc, the predicted primary HULISc concentrations were set to equal
348 the observed HULISc and the secondary HULISc were set to zero. Based on the HULIS emissions from residential
349 biofuel and coal burning described in Section 3.3, the contributions of biofuel and coal burning in the residential sector
350 to ambient HULIS were estimated separately.

351 Overall, residential biofuel burning was the most important source of ambient HULIS, contributing nearly half of the
352 ambient HULIS concentrations, much higher than those results from the PRD in Southern China (less than 20%)
353 (Kuang et al. 2015). This difference is likely with greater biofuel burning during the heating seasons in the Beijing area.
354 Residential coal burning contributes $15.1 \pm 2.9\%$ to ambient HULIS and is also a significant source of ambient HULIS.
355 Great contribution from residential sector to ambient HULIS is consistent with the estimation of HULIS primary
356 emission and the correlations between HULIS and primary species previously presented. Vehicle emissions and other
357 primary sources, such as industries, contribute negligible amounts to the ambient HULIS. Contributions from the
358 residential sector display strong seasonal variations. In winter and spring, residential biofuel and coal burning accounted
359 for about 80% of the total HULISc while their contributions were reduced to approximately 40% in summer and
360 autumn. The seasonal variations were a reflection of seasonal pattern of those activities in this region.
361 Secondary formation is estimated to have contributed an average of $38.9 \pm 9.1\%$ to the HULIS concentrations and was
362 another major source to ambient HULIS. However, our result is much lower than those results from PRD in Southern
363 China (55 to 69%) (Kuang et al. 2015). The difference is driven by the differences in sources and climatological
364 patterns between these two sites. There is much greater combustion for space heating in the colder north and
365 atmospheric reaction rates will be higher in the warmer south. Contribution from secondary processes also shows
366 obvious seasonal variations trend. In winter and spring, secondary processes accounted for 25% to 30% of the total
367 HULISc with large uncertainties while their contributions were increased to $50.2 \pm 19.3\%$ and $63.2 \pm 18.3\%$ in summer
368 and autumn. Higher secondary contributions were also found during warm seasons in the PRD region (Kuang et al.
369 2015). In addition to the proposed heterogeneous secondary formation pathways for HULISc, oxidation reactions
370 initiated by chlorine (Cl) radicals can form SOA (Wang and Ruiz, 2017; Riva et al., 2015). Thus, Cl release by coal
371 combustion may have the potential to contribute to HULISc, especially during winter when OH radical concentrations
372 are much lower (monthly average 5.5×10^{-3} ppt for winter vs. 1.25×10^{-1} ppt for summer based on CMAQ calculations
373 for Beijing). However, the concentrations of secondary HULISc for winter estimated in this study are uncertain ($1.8 \pm$
374 $2.2 \mu\text{g m}^{-3}$) compared to the summer time average concentration ($1.0 \pm 0.4 \mu\text{g m}^{-3}$). Therefore, the role of Cl initiated
375 reactions producing HULISc cannot be definitively determined.

376 Figure 4 shows the scatter plot of predicted primary HULISc vs observed HULISc concentrations. Moderate to strong
377 correlations between predicted primary HULISc and observed HULISc were observed in winter and spring, while
378 relatively weaker correlations were found in autumn. Moreover, low correlations were observed in summer. The variation
379 of correlations between predicted primary HULISc and observed HULISc in different seasons also provides additional
380 support for the relative importance of primary and secondary HULIS as shown in Table 3.

381 **Supporting Information**

382 The supporting information file for this paper provides the details of HULIS analytical procedures, and prior literature
383 regarding HULIS in the ambient aerosol. It also provides some additional figures and descriptions that help to support
384 the analyses and discussion presented in the paper.

385 **Author contributions**

386 XL designed the experiments and analyzed the data and wrote the paper. JH collected and analyzed the samples. PKH
387 provided advice, supervision, and feedback throughout the drafting and submission process. JH provided samples from
388 vehicle emissions. QS analyzed the samples. QC collected the samples. QY conducted the CMAQ modeling and wrote
389 the paper.

390 **Acknowledgment**

391 This work was supported by the National Nature Science Foundation of China (Grant No. 41575119, 41275121) and the
392 National Key Research and Development Program of China (No. 2017YFC0211404). The authors also want to
393 acknowledge the Texas A&M Supercomputing Facility (<http://sc.tamu.edu>) for providing computing resources useful in
394 conducting the CMAQ simulations reported in this paper.

395 **References**

- 396 Appel, K.W., Pouliot, G.A., Simon, H., Sarwar, G., Pye, H.O.T., Napelenok, S.L., Akhtar, F., and Roselle, S.J.:
397 Evaluation of dust and trace metal estimates from the Community Multiscale Air Quality (CMAQ) model version
398 5.0, *Geosci. Model Dev.*, 6, 883–899, 2013.
- 399 Baduel, C., Voisin, D., and Jaffrezo, J. L.: Seasonal variations of concentrations and optical properties of water soluble
400 HULIS collected in urban environments, *Atmos. Chem. Phys.*, 10, 4085–4095, 2010.
- 401 Beine, H., Anastasio, C., Esposito, G., Patten, K., Wilkening, E., Domine, F., Voisin, D., Barret, M., Houdier, S., and
402 Hall, S.: Soluble, light absorbing species in snow at Barrow, Alaska, *J. Geophys. Res.*, 116, D00R05,
403 doi:10.1029/2011JD016181, 2011.
- 404 Cheng, Y., Engling, G., He, K.B., Duan, F.K., Ma, Y.L., Du, Z.Y., Liu, J.M., Zheng, M., and Weber, R.J.: Biomass
405 burning contribution to Beijing aerosol, *Atmos. Chem. Phys.*, 13, 7765–7781, 2013.
- 406 Chow, J.C., Watson, J.G., Chen, L.W.A., Chang, M.C.O., Robinson, N.F., Trimble D., and Kohl, S.: The IMPROVE-A

407 temperature protocol for thermal/optical carbon analysis: maintaining consistency with a long-term database, *J. Air*
408 *Waste Manage.*, 57, 1014–1023, 2007.

409 Dinar, E., Taraniuk, I., Graber, E.R., Katsman, S., Moise, T., Anttila, T., Mentel, T.F., and Rudich, Y.: Cloud
410 condensation nuclei properties of model and atmospheric HULIS, *Atmos. Chem. Phys.*, 6, 2465–2481, 2006.

411 El Haddad, I., Marchand, N., Dron, J., Temime-Roussel, B., Quivet, E., Wortham, H., Jaffrezo, J.-L., Baduel, C., Voisin,
412 D., Besombes, J., and Gille, G.: Comprehensive primary particulate organic characterization of vehicular exhaust
413 emissions in France, *Atmos. Environ.*, 43, 6190–6198, 2009.

414 Fan, X., Wei, S., Zhu, M., Song, J., and Peng, P.: Comprehensive characterization of humic-like substances in smoke
415 $PM_{2.5}$ emitted from the combustion of biomass materials and fossil fuels, *Atmos. Chem. Phys.*, 16, 13321–13340,
416 2016.

417 Fan, X.J., Song, J.Z., and Peng, P.A.: Comparison of isolation and quantification methods to measure humic-like
418 substances (HULIS) in atmospheric particles, *Atmos. Environ.*, 60, 366–374, 2012.

419 Feczko, T., Puxbaum, H., Kasper-Giebl, A., Handler, M., Limbeck, A., Gelencsér, A., Pio, C., Preunkert, S., and
420 Legrand, M.: Determination of water and alkaline extractable atmospheric humic-like substances with the TU
421 Vienna HULIS analyzer in samples from six background sites in Europe, *J. Geophys. Res.*, 112, D23S10, 2007.

422 France, J.L., King, M.D., Frey, M.M., Erbland, J., Picard, G., Preunkert, S., MacArthur, A., and Savarino, J.: Snow
423 optical properties at Dome C (Concordia), Antarctica, implications for snow emissions and snow chemistry of
424 reactive nitrogen, *Atmos. Chem. Phys.*, 11, 9787–9801, 2011.

425 France, J.L., Reay, H.J., King, M.D., Voisin, D., Jacobi, H.W., Domine, F., Beine, H., Anastasio, C., MacArthur, A., and
426 Lee-Taylor, J.: Hydroxyl radical and NO_x production rates, black carbon concentrations and light-absorbing
427 impurities in snow from field measurements of light penetration and nadir reflectivity of onshore and offshore
428 coastal Alaskan snow, *J. Geophys. Res.*, 117, D00R12, 2012.

429 Gao, J., Tian, H., Cheng, K., Lu, L., Zheng, M., Wang, S., Hao, J., Wang, K., Hua, S., Zhu, C., and Wang, Y.: The
430 variation of chemical characteristics of $PM_{2.5}$ and PM_{10} and formation causes during two haze pollution events in
431 urban Beijing, China, *Atmos. Environ.*, 107, 1–8, 2015.

432 Gao, J.J., Tian, H.Z., Chen, K., Wang, Y.X., Wu, Y. and Zhu, C.Y.: Seasonal and spatial variation of trace elements in
433 multi-size airborne particulate matters of Beijing, China: Mass concentration, enrichment characteristics, source
434 apportionment, chemical speciation and bioavailability, *Atmos. Environ.*, 99: 257–265, 2014.

435 Ghio, A. J., Stonehuerner, J., Pritchard, R. J., Piantadosi, C. A., Quigley, D. R., Dreher, K. L., and Costa, D. L.:
436 Humic-like substances in air pollution particulates correlate with concentrations of transition metals and oxidant

437 generation, *Inhalation Toxicol.*, 8, 479–494, 1996.

438 Goncalves, C., Alves, C., Evtyugina, M., Mirante, F., Pio, C., Caseiro, A., Schmidl, C., Bauer, H., and Carvalho F.:
439 Characterisation of PM₁₀ emissions from woodstove combustion of common woods grown in Portugal, *Atmos.*
440 *Environ.*, 44(35): 4474-4480, 2010.

441 Graber, E.R. and Rudich, Y.: Atmospheric HULIS: How humic-like are they? A comprehensive and critical review,
442 *Atmos. Chem. Phys.*, 6, 729-753, 2006.

443 Gysel, M., Weingartner, E., Nyeki, S., Paulsen, D., Baltensperger, U., Galambos, I., and Kiss, G.: Hygroscopic
444 properties of water-soluble matter and humic-like organics in atmospheric fine aerosol, *Atmos. Chem. Phys.*, 4,
445 35-50, 2004.

446 He L. Q., Hu J. N., and Zu L.: Emission characteristics of exhaust PM_{2.5} and its carbonaceous components from China
447 to China heavy-duty diesel vehicles, *Acta Scientiae Circumstantiae*, 35(3), 656-662, 2015 (in Chinese).

448 Hoffer, A., Gelencsér, A., Guyon, P., Kiss, G., Schmid, O., Frank, G. P., Artaxo, P., and Andreae, M. O.: Optical
449 properties of humic-like substances (HULIS) in biomass-burning aerosols, *Atmos. Chem. Phys.*, 6, 3563–3570,
450 2006.

451 Hu, J., Wu, L., Zheng, B., Zhang, Q., He, K., Zhang, Q., Li, X., Yang, F., Ying Q., and Zhang, H.: Source contributions
452 and regional transport of primary particulate matter in China, *Environ. Pollut.*, 207, 31-42, 2015.

453 Jiang, Q., Sun, Y.L., Wang, Z., and Yin, Y.: Aerosol composition and sources during the Chinese Spring Festival:
454 fireworks, secondary aerosol, and holiday effects, *Atmos. Chem. Phys.*, 15, 6023-6034, 2015.

455 Jing, H., Li, Y.F., Zhao, J.T., Li, B., Sun, J.L., Chen, R., Gao, Y.X., and Chen, C.Y.: Wide-range particle characterization
456 and elemental concentration in Beijing aerosol during the 2013 Spring Festival, *Environ. Pollut.*, 192, 204-211,
457 2014.

458 Kelly, J.T., Bhave, P.V., Nolte, C.G., Shankar, U., and Foley, K.M.: Simulating emission and chemical evolution of
459 coarse sea-salt particles in the Community Multiscale Air Quality (CMAQ) model, *Geosci. Model Dev.* 3, 257-273,
460 2010.

461 Kiss, G., Varga, B., Galambos, I., and Ganszky, I.: Characterization of water-soluble organic matter isolated from
462 atmospheric fine aerosol, *J. Geophys. Res.*, 107, 8339, 2002.

463 Krivácsy, Z., Gelencsér, A., Kiss, G., Mészáros, E., Molnár, Á., Hoffer, A., Mészáros, T., Sárvári, Z., Temesi, D.,
464 Varga, B., Baltensperger, U., Nyeki, S., and Weingartner, E.: Study on the chemical character of water soluble
465 organic compounds in fine atmospheric aerosol at the Jungfrauoch, *J. Atmos. Chem.*, 39, 235-259, 2001.

466 Krivácsy, Z., Kiss, G., Ceburnis, D., Jennings, G., Maenhaut, W., Salma, I., and Shooter, D.: Study of water-soluble

467 atmospheric humic matter in urban and marine environments, *Atmos. Res.*, 87, 1-12, 2008.

468 Kuang, B. Y., Lin, P., Huang, X. H. H., and Yu, J. Z.: Sources of humic-like substances in the Pearl River Delta, China:
469 positive matrix factorization analysis of PM_{2.5} major components and source markers, *Atmos. Chem. Phys.*, 15,
470 1995-2008, 2015.

471 Li, Q., Jiang, J., Qi, J., Deng, J., Yang, D., Wu, J., Duan, L., and Hao, J.: Improving the energy efficiency of stoves to
472 reduce pollutant emissions from household solid fuel combustion in China, *Environ. Sci. Technol. Lett.*, 3,
473 369-374, 2016.

474 Li, X., Wang, S., Duan, L., Hao, J., and Nie, J.: Carbonaceous aerosol emissions from household biofuel combustion in
475 China, *Environ. Sci. Technol.*, 43: 6076-6081, 2009.

476 Li, X., Wang, S., Duan, L., Hao, J., Li, C., Chen, Y., and Yang, L.: Particulate and trace gas emissions from open
477 burning of wheat straw and corn stover in China, *Environ. Sci. Technol.*, 41, 6052-6058, 2007.

478 Li, Y., Li, Z., and Hu, J.: Emission profile of exhaust PM_{2.5} from light-duty gasoline vehicles, *Research of
479 Environmental Sciences*, 29(4): 503-508, 2016 (in Chinese).

480 Lim, H. J. and Turpin, B. J.: Origins of primary and secondary organic aerosol in Atlanta: Results' of time-resolved
481 measurements during the Atlanta supersite experiment, *Environ. Sci. Technol.*, 36, 4489-4496, 2002.

482 Lin, P. and Yu, J.Z.: Generation of reactive oxygen species mediated by humic-like substances in atmospheric aerosols,
483 *Environ. Sci. Technol.*, 45, 10362-10368, 2011.

484 Lin, P., Engling, G., and Yu, J.Z.: Humic-like substances in fresh emissions of rice straw burning and in ambient
485 aerosols in the Pearl River Delta Region, China. *Atmos. Chem. Phys.*, 10, 6487-6500, 2010.

486 Lin, P., Huang, X.F., He, L.Y., and Yu, J.Z.: Abundance and size distribution of HULIS in ambient aerosols at a rural
487 site in South China, *J. Aerosol Sci.*, 41, 74-87, 2010.

488 Lin, P., Rincon, A.G., Kalberer, M., and Yu, J.Z.: Elemental Composition of HULIS in the Pearl River Delta Region,
489 China: Results inferred from positive and negative electrospray high resolution mass spectrometric data, *Environ.
490 Sci. Technol.*, 46, 7454-7462, 2012.

491 Lipsky, E. M., and Robinson, A. L.: Effects of dilution on fine particle mass and partitioning of semivolatile organics in
492 diesel exhaust and wood smoke, *Environ. Sci. Technol.*, 40(1), 155-162, 2006.

493 Liu, J., Mauzerall, D. L., Chen, Q., Zhang, Q., Song, Y., Peng, W.; Klimont, Z., Qiu, X., Zhang, S., Hu, M., Lin, W.,
494 Smith, K.R., and Zhu, T.: Air pollutant emissions from Chinese households: A major and underappreciated
495 ambient pollution source, *Proc. Natl. Acad. Sci. USA*, 113, 28, 7756-7761, 2016.

496 Marotta, A., Pavlovic J., Ciuffo, B., Serra, S., Fontaras, G.: Gaseous emissions from light-duty vehicles: moving from

497 NEDC to the new WLTP test procedure, *Environ. Sci. Technol.*, 49 (14), 8315–8322, 2015.

498 May, A. A., Levin, E. J. T., Hennigan, C. J., Riipinen, I., Lee, T., Collett, J. L., Jimenez, J. L., Kreidenweis, S. M.,
499 Robinson, A. L.: Gas-particle partitioning of primary organic aerosol emissions: 3. Biomass burning, *Journal of*
500 *Geophysical Research-Atmospheres*, 118(19): 11327-11338, 2013.

501 Ministry of Environment Protection of China: Technical guide for the compilation of emission inventory for
502 atmospheric fine particulates, 2014 (in Chinese).

503 Nguyen, Q.T., Kristensen, T.B., Hansen, A.M.K., Skov, H., Bossi, R., Massling, A., Sørensen, L.L., Bilde, M., Glasius,
504 M., Nøjgaard, J.K.: Characterization of humic-like substances in Arctic aerosols, *J. Geophys. Res.*, 119, 5011-5027,
505 2014.

506 Park, S. S. and Yu, J.: Chemical and light absorption properties of humic-like substances from biomass burning
507 emissions under controlled combustion experiments, *Atmos. Environ.*, 136, 114-122, 2016.

508 Park, S.S., Cho, S.Y., and Bae, M.S.: Source identification of water-soluble organic aerosols at a roadway site using a
509 positive matrix factorization analysis, *Sci. Total Environ.*, 533, 410-421, 2015.

510 Park, S.S., Cho, S.Y., Kim, K.W., Lee, K.H., and Jung, K.: Investigation of organic aerosol sources using fractionated
511 water-soluble organic carbon measured at an urban site. *Atmos. Environ.*, 55, 64-72, 2012.

512 Pavlovic, J. and Hopke, P.K.: Chemical nature and molecular weight distribution of the water-soluble fine and ultrafine
513 PM fractions collected in a rural environment, *Atmos. Environ.*, 59, 264-271, 2012.

514 Pio, C.A., Legrand, M., Alves, C.V., Oliveira, T., Afonso, J., Caseiro, A., Puxbaum, H., Sanchez-Ochoa, A., and
515 Gelencsér, A.: Chemical composition of atmospheric aerosols during the 2003 summer intense forest fire period,
516 *Atmos. Environ.*, 42, 7530-7543, 2008.

517 Riva, M., Healy, R.M., Flaud, P.-M., Perraudin, E., Wenger, J.C., Villenave, E.: Gas- and particle-phase products from
518 the chlorine-initiated oxidation of polycyclic aromatic hydrocarbons, *J. Phys. Chem. A* 119, 11170-11181, 2015.

519 Salma, I., Mészáros, T., and Maenhaut, W.: Mass size distribution of carbon in atmospheric humic-like substances and
520 water soluble organic carbon for an urban environment, *J. Aerosol Sci.*, 56, 53-60, 2013.

521 Salma, I., Mészáros, T., Maenhaut, W., Vass, E., and Majer, Z.: Chirality and the origin of atmospheric humic-like
522 substances, *Atmos. Chem. Phys.*, 10, 1315-1327, 2010.

523 Salma, I., Ocskay, R., and Láng, G.G.: Properties of atmospheric humic-like substances – water system, *Atmos. Chem.*
524 *Phys.*, 8, 2243-2254, 2008.

525 Salma, I., Ocskay, R., Chi, X.G., and Maenhaut, W.: Sampling artefacts, concentration and chemical composition of fine
526 water-soluble organic carbon and humic-like substances in a continental urban atmospheric environment, *Atmos.*

527 Environ., 41, 4106-4118, 2007.

528 Schmidl, C., Bauer, H., Dattler, A., Hitzenberger, R., Weissenboeck, G., Marr, I. L., and Puxbaum, H.: Chemical
529 characterisation of particle emissions from burning leaves, *Atmos. Environ.*, 42, 9070–9079, 2008.

530 Schmidl, C., Marr, L. L., Caseiro, A., Kotianova, P., Berner, A., Bauer, H., Kasper-Giebl, A., and Puxbaum, H.
531 Chemical characterisation of fine particle emissions from wood stove combustion of common woods growing in
532 mid-European Alpine regions, *Atmos. Environ.*, 42, 126–141, 2008.

533 Shen, Z.X., Cao, J.J., Arimoto, R., Han, Z.W., Zhang, R.J., Han, Y.M., Liu, S.X., Okuda, T., Nakao, S., and Tanaka, S.:
534 Ionic composition of TSP and PM_{2.5} during dust storms and air pollution episodes at Xi'an, China, *Atmos.*
535 *Environ.*, 43, 2911-2918, 2009.

536 Song, J.Z., He, L.L., Peng, P.A., Zhao, J.P., and Ma, S.X. Chemical and isotopic composition of humic-like substances
537 (HULIS) in ambient aerosols in Guangzhou, South China, *Aerosol Sci. Technol.*, 46, 533-546, 2012.

538 Srivastava, D., Tomaz, S., Favez, O., Lanzafame, G. M., Golly, B., Besombes, J.-L., Alleman, L. Y., Jaffrezo, J.-L.,
539 Jacob, V., Perraudin, E., Villenave E., and Albinet, A.: Speciation of organic fraction does matter for source
540 apportionment. Part 1: A one-year campaign in Grenoble (France), *Sci. Total Environ.*, 624, 1598–1611, 2018.

541 Sun, Y., Du, W., Fu, P., Wang, Q., Li, J., Ge, X., Zhang, Q., Zhu, C., Ren, L., and Xu, W.: Primary and secondary
542 aerosols in Beijing in winter: sources, variations and processes, *Atmos. Chem. Phys.*, 16 (13), 8309–8329, 2016.

543 Tan, J., Xiang, P., Zhou, X., Duan, J., Ma, Y., He, K., Cheng, Y., Yu, J., and Querol, X.: Chemical characterization of
544 humic-like substances (HULIS) in PM_{2.5} in Lanzhou, China. *Sci. Total Environ.*, 573, 1481-1490, 2016.

545 Turpin, B. J. and Huntzicker, J. J.: Identification of Secondary Organic Aerosol Episodes and Quantitation of Primary
546 and Secondary Organic Aerosol Concentrations during SCAQS., *Atmos. Environ.*, 29, 3527–3544, 1995.

547 Varga, B., Kiss, G., Ganszky, I., Gelencser, A., and Krivacsy, Z.: Isolation of water-soluble organic matter from
548 atmospheric aerosol, *Talanta*, 55, 561–572, 2001.

549 Verma, V., Rico-Martinez, R., Kotra, N., King, L., Liu, J. M., Snell, T. W., and Weber, R. J.: Contribution of
550 water-soluble and in-soluble components and their hydrophobic/hydrophilic sub-fractions to the reactive oxygen
551 species-generating potential of fine ambient aerosols, *Environ. Sci. Technol.*, 46, 11384–11392, 2012.

552 Voliotis, A., Prokes R., Lammel, G., and Samara C. New insights on humic-like substances associated with wintertime
553 urban aerosols from central and southern Europe: Size-resolved chemical characterization and optical properties,
554 *Atmos. Environ.*, 166, 286-299, 2017.

555 Wang, B. and Knopf D. A.: Heterogeneous ice nucleation on particles composed of humic-like substances impacted by
556 O₃, *J. Geophys. Res.*, 116, D03205, doi:10.1029/2010JD014964, 2011.

557 Wang, D. S., Liu, M. R., Bai, X. F., and Ding, H.: The situation analysis of civil coal in the Beijing-Tianjin-Hebei
558 Region, *Technology of Coal*, 3, 47-50, 2016 (in Chinese).

559 Wang, D.S., Ruiz, L.H.: Secondary organic aerosol from chlorine-initiated oxidation of isoprene, *Atmos. Chem. Phys.*
560 17, 13491-13508, 2015.

561 Wang, H., Tian, M., Li, X., Chang, Q., Cao, J., Yang, F., Ma, Y., and He, K.: Chemical composition and light extinction
562 contribution of PM_{2.5} in urban Beijing for a 1-year period, *Aerosol Air Qual. Res.*, 15, 2200–2211, 2015.

563 Wang, Q., Shao, M., Zhang, Y., Wei, Y., Hu, M., and Guo, S.: Source apportionment of fine organic aerosols in Beijing.
564 *Atmos. Chem. Phys.*, 9, 8573–8585, 2009.

565 Wang, Y., Hopke, P.K., Rattigan, O.V., Chalupa, D.C., and Utell, M.J.: Source apportionment of airborne particulate
566 matter using inorganic and organic species as tracers, *Atmos. Environ.*, 55, 525–532, 2012.

567 Wang, Y., Hopke, P.K., Rattigan, O.V., Xia, X., Chalupa, D.C., and Utell, M.J.: Characterization of residential wood
568 combustion particles using the two-wavelength aethalometer, *Environ Sci. Technol.*, 45, 7387–7393, 2011.

569 Wiedinmyer, C., Akagi, S.K., Yokelson, R.J., Emmons, L.K., Al-Saadi, J.A., Orlando, J.J., and Soja, A.J.: The Fire
570 INventory from NCAR (FINN): a high resolution global model to estimate the emissions from open burning,
571 *Geosci. Model Dev.*, 4, 625-641, 2011.

572 Yao, X., Chan, C. K., Fang, M., Cadle, S., Chan, T., Mulawac, P., He K., and Ye, B.: The water-soluble ionic
573 composition of PM_{2.5} in Shanghai and Beijing, China, *Atmos. Environ.*, 36, 4223–4234, 2002.

574 Ying, Q., Feng, M., Song, D., Wu, L., Hu, J., Zhang, H., Kleeman, M.J., and Li, X.: Improve regional distribution and
575 source apportionment of PM_{2.5} trace elements in China using inventory-observation constrained emission factors,
576 *Sci. Total Environ.*, 624, 355-365, 2018.

577 Yu, L., Wang, G., Zhang, R., Zhang, L., Song, Y., Wu, B., Li, X., An, K., and Chu, J.: Characterization and source
578 apportionment of PM_{2.5} in an urban environment in Beijing, *Aerosol Air Qual. Res.*, 13, 574-583, 2013.

579 Zhang, R., Jing, J., Tao, J., Hsu, S. C., Wang, G., Cao, J., Lee, C. S. L., Zhu, L., Chen, Z., Zhao, Y., and Shen, Z.:
580 Chemical characterization and source apportionment of PM_{2.5} in Beijing: seasonal perspective, *Atmos. Chem.*
581 *Phys.*, 13, 7053-7074, 2013.

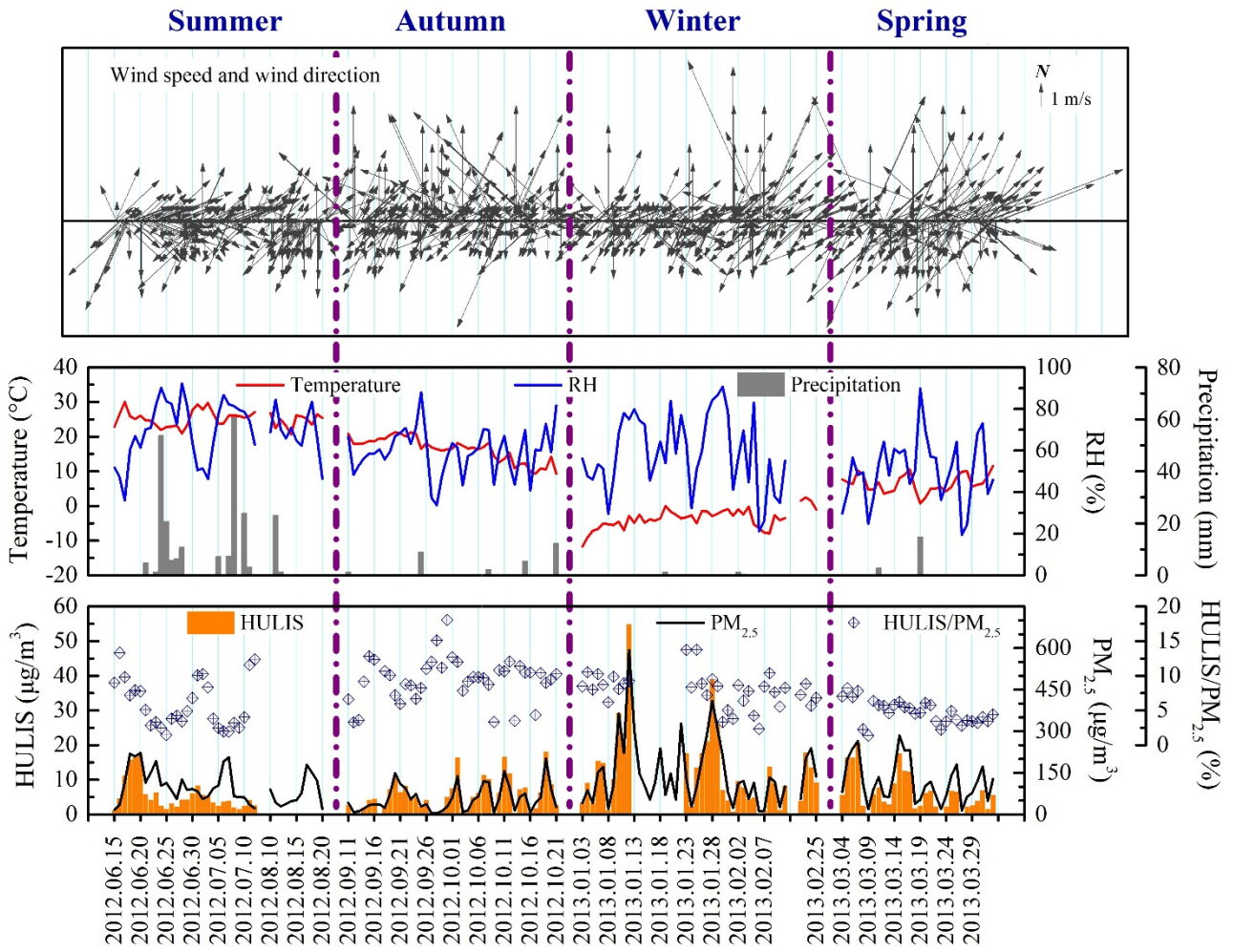
582 Zhang, Y. M., Wang, Y. Q., Zhang, X. Y., et al.: Chemical components, variation, and source identification of PM₁
583 during the heavy air pollution episodes in Beijing in December 2016. *J. Meteor. Res.*, 32(1), 1–13, doi:
584 10.1007/s13351-018-7051-8, 2018.

585 Zhao, M.F., Huang, Z.S., Qiao, T., Zhang, Y.K., Xiu, G.L., and Yu, J.Z.: Chemical characterization, the transport
586 pathways and potential sources of PM_{2.5} in Shanghai: Seasonal variations, *Atmos. Res.*, 158-159, 66-78, 2015.

587 Zheng, G. J., Duan, F.K., Su, H., Ma, Y.L., Cheng, Y., Zheng, B., Zhang, Q., Huang, T., Kimoto, T., Chang, D., Pöschl,
588 U., Cheng, Y. F., and He, K. B.: Exploring the severe winter haze in Beijing: the impact of synoptic weather,
589 regional transport and heterogeneous reactions, *Atmos. Chem. Phys.*, 15, 2969-2983, 2015.

590 Zheng, G. J., He, K.B., Duan, F.K., Cheng, Y., and Ma, Y. L.: Measurement of humic-like substances in aerosols: A
591 review, *Environ. Pollut.*, 181, 301-314, 2013.

592

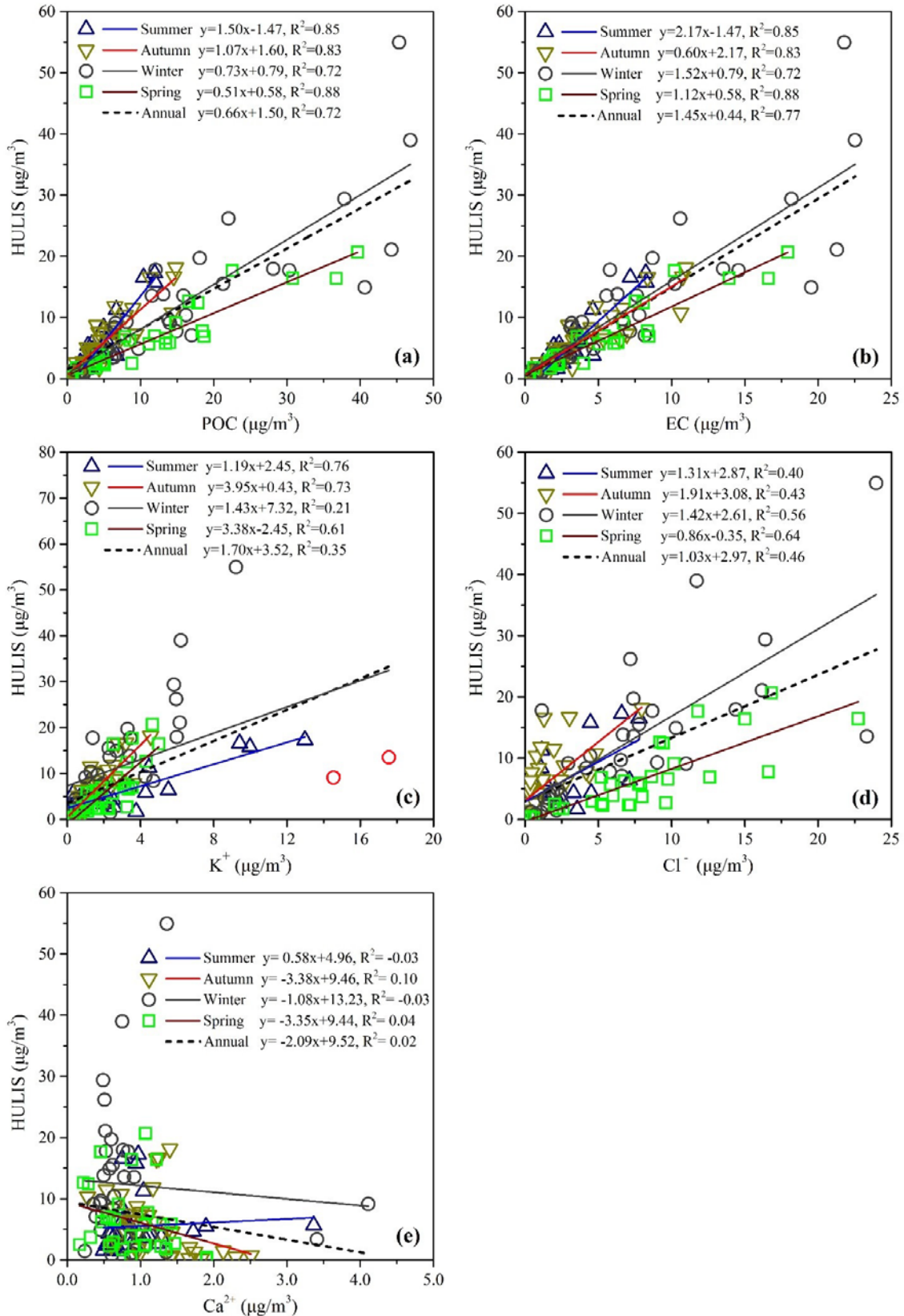


594

595 **Figure 1.** Time series of meteorological data (wind speed, wind direction, temperature, relative humidity and
 596 precipitation), HULIS, PM_{2.5} and HULIS/PM_{2.5} for the sampling period.

597

598



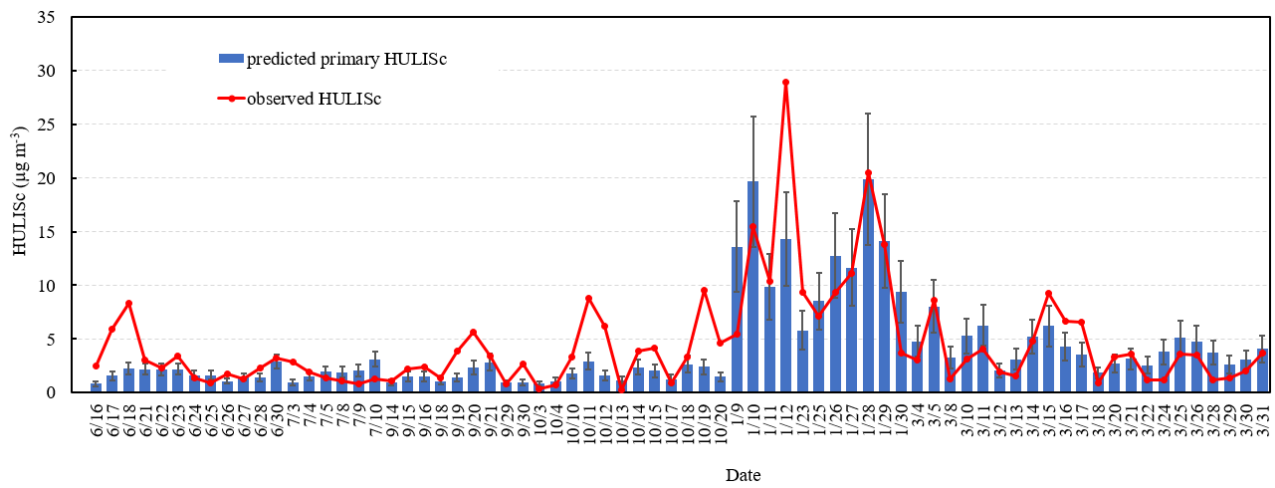
600

601

602

603

Figure 2. Correlations between HULIS and POC (a), HULIS & EC (b), HULIS & K^+ (c), HULIS & Cl^- (d), HULIS & Ca^{2+} (e). Concentrations in four seasons are represented by different shapes with different colors. Linear regressions are also given with corresponding equations.



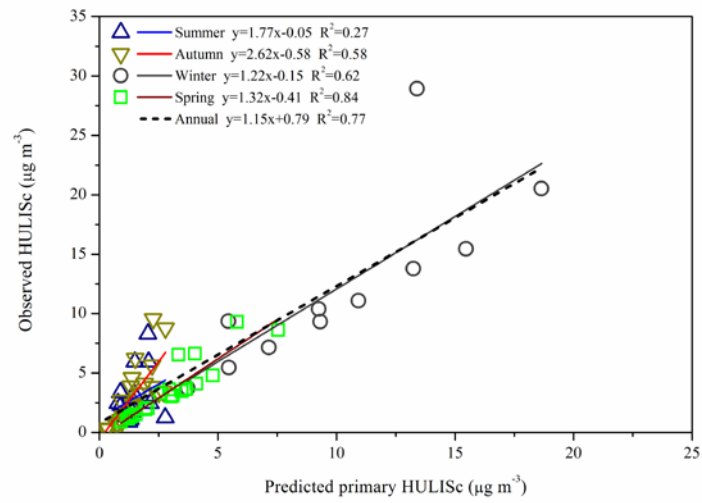
604

605 **Figure 3.** Predicted primary HULISc and observed HULISc concentrations on the days with relatively good primary

606 PM_{2.5} model performance. Error bar is the standard deviation of prediction, which is calculated as described in SI Text

607 S3.1.

608



610

611 **Figure 4.** Scatter plot of predicted primary HULISc and observed HULISc concentrations. Concentrations of different
 612 seasons are represented by different shapes with different colors. Linear regressions are also given with corresponding
 613 equations.

614

615 **Tables**

616 **Table 1.** Summary of the concentrations of PM_{2.5}, carbon species, water-soluble ions and percentages of several
 617 compounds to some others.

Species	Average	Summer	Autumn	Winter	Spring
	Average ± SD	Average ± SD	Average ± SD	Average ± SD	Average ± SD
PM _{2.5} (μg/m ³)	106±89	98 ± 60	58±48	150±121	120±76
OC (μg/m ³)	16.0±15.8	8.5±5.2	10.3±7.4	28.9±22.0	14.6±10.8
EC (μg/m ³)	5.0±4.8	3.3±1.8	3.5±2.9	7.8±6.6	5.3±4.7
OC/EC	3.6±1.4	2.8±0.8	3.8±1.9	4.3±1.2	3.3±0.9
WSOC (μg/m ³)	6.5±6.5	4.4±3.6	5.2±4.0	10.3±9.8	5.9±4.9
HULIS (μg/m ³)	7.5±7.8	5.5±4.4	5.6±4.7	12.3±11.7	6.5±5.5
HULIS/PM _{2.5} (%)	7.2±3.3	5.9±3.5	9.4±3.1	7.9±2.5	4.8±1.7
HULIS _C /OC (%)	24.5±8.3	29.2±6.2	26.2±9.6	21.0±7.1	22.0±6.9
HULIS _C /WSOC (%)	59.5±9.2	66.7±5.4	54.1±11.2	62.3±5.7	56.6±6.3
SO ₄ ²⁻ (μg/m ³)	22.3±24.1	22.6±17.0	10.9±13.2	32.7±35.1	22.5±16.5
NO ₃ ⁻ (μg/m ³)	18.6±18.0	17.2±13.4	10.8±13.2	20.1±17.8	29.0±23.8
Cl ⁻ (μg/m ³)	4.2±4.9	1.8±1.9	1.3±1.6	6.5±5.7	7.9±5.2
Na ⁺ (μg/m ³)	0.60±0.51	0.40±0.30	0.33±0.41	0.89±0.61	0.79±0.36
K ⁺ (μg/m ³)	2.2±2.6	2.2±2.9	1.3±1.0	3.2±3.6	2.2±1.3
Mg ²⁺ (μg/m ³)	0.18±0.19	0.15±0.07	0.18±0.08	0.24±0.32	0.10±0.07
Ca ²⁺ (μg/m ³)	0.97±0.57	0.99±0.52	1.14±0.48	0.83±0.70	0.89±0.46
NH ₄ ⁺ (μg/m ³)	14.1±13.0	13.2±9.8	6.6±7.0	19.1±16.9	18.4±11.8

618

619

620 **Table 2.** HULIS_C/OC and HULIS_C/WSOC values in the source samples

Source type	Stove/vehicle	HULIS _C /OC	HULIS _C /WSOC	n
Residential biofuel burning				
wood burning	improved stove	0.41±0.07	0.62±0.06	3
wheat straw	improved stove	0.50±0.04	0.65±0.05	4
corn stover	improved stove	0.42±0.04	0.62±0.04	3
Residential chunk coal combustion				
SM, Var=32.4%	high efficiency heating stove	0.14±0.07	0.51±0.04	3
JY, Var=27.7%	high efficiency heating stove	0.18±0.04	0.50±0.04	3
BH, Var=25.0%	high efficiency heating stove	0.08±0.02	0.44±0.01	3
DT, Var=19.4%	high efficiency heating stove	0.15	0.62	1
SM, Var=32.4%	traditional cooking and heating stove	0.06±0.01	0.46±0.02	3
JY, Var=27.7%	traditional cooking and heating stove	0.07±0.03	0.41±0.06	3
BH, Var=25.0%	traditional cooking and heating stove	0.05±0.01	0.43±0.08	3
Residential briquette coal combustion				
XM, Var=9.6%	high efficiency heating stove	0.24±0.07	0.53±0.09	3
Vehicle exhaust				
traffic tunnel	mixture of gasoline and diesel vehicles	0.05	0.65	1
heavy-duty diesel trucks	Euro II	0.16±0.02	0.38±0.03	3
light-duty gasoline vehicles	Euro IV	0.11±0.03	0.21±0.11	4

621 Note: SM, DT indicate that coals come from the coal mines in ShenMu of Shaanxi Province and DaTong of Shanxi
622 Province in China, respectively. JY and BH were supplied by two companies with the name of JiuYang and BeiHua,
623 respectively, and no producing area of coal were not available. XM indicates briquette coal, which is the abbreviation of
624 briquette coal in Chinese (XingMei).

625

626

627

628 **Table 3.** Average and seasonal contributions percent of various sources to ambient HULIS concentrations in Beijing
 629 (%)

	Residential biofuel burning	Residential coal burning	Transportation	Industries	Biomass open burning	Secondary process
Annual	47.1±6.5	15.1±2.9	2.0±0.3	1.3±0.3	1.7±0.5	38.9±9.1
Summer	29.2±6.5	9.4±2.7	3.9±1.1	2.9±1.2	10.3±3.7	50.2±19.3
Autumn	24.8±5.5	8.0±2.3	2.7±0.8	1.7±0.8	1.1±0.6	63.2±18.3
Winter	55.7±14.1	17.9±6.3	1.1±0.4	0.6±0.3	0.0±0.0	30.3±17.2
Spring	62.7±12.8	20.1±5.4	2.0±0.5	1.2±0.4	0.1±0.1	25.4±13.3

630 Note: only the sources with an average contribution over 1% were provided. Uncertainty estimation for the seasonal
 631 and annual primary and secondary HULIS contributions was determined using a bootstrap sampling technique, which
 632 is described in Text S3.2. These uncertainties are based on the assumption that the uncertainty of the $PPM_{2.5}$ and f_{OC}
 633 values are 30% and 15%, respectively. Uncertainty calculations based on larger uncertainties (50% for both $PPM_{2.5}$ and
 634 f_{OC}) show 5-10% higher relative uncertainties for the residential biofuel and secondary process but small changes for
 635 other primary sectors (see Table S5).